Ecosystems (2019) 22: 677–698
https://doi.org/10.1007/s10021-018-0295-4

ECOSYSTEMS

© 2018 Springer Science+Business Media, LLC, part of Springer Nature

Quantifying the Uncertainty in Modeled Water Drainage and Nutrient Leaching Fluxes in Forest Ecosystems

Gregory van der Heijden,[1]* Armand Hinz,[1] Serge Didier,[1] Claude Nys,[1] Etienne Dambrine,[2] and Arnaud Legout[1]

[1]*INRA UR 1138 BEF, route d'amance, 54280 Champenoux, France;* [2]*INRA UMR CARRTELL (INRA-Univ Savoie), 73376 Le Bourget-du-Lac, France*

Abstract

In terrestrial ecosystem studies, water drainage and nutrient leaching in the soil profile are estimated with hydrological models. Comparing modeled results to empirical data or comparing data from different models is, however, difficult because the uncertainty of input–output budget predictions is often unknown. In this study, we developed a procedure combining a Generalized Likelihood Uncertainty Estimation and a Monte-Carlo modeling approach to estimate uncertainty in model parameter estimates and model outputs water drainage and nutrient leaching fluxes for the WatFor water balance model. This procedure was then applied to compare different model optimization strategies (daily soil moisture measurements, monthly measurements of chloride concentrations in soil solution, and the elution of a concentrated chloride) at the same experimental site in a 90-year-old European beech (*Fagus sylvatica* L.) forest in Brittany (France). We show that the monitoring data of natural variations of chloride concentrations in soil solution were the most efficient dataset to calibrate the WatFor model compared to the soil moisture and chloride tracing experimental data. We also show that water tracing experimental data are the most efficient data to estimate the preferential flow generation model parameters. The optimization strategy had little influence on the predicted water drainage flux and nutrient leaching flux at the root zone boundary on a yearly time scale but influenced water and nutrient fluxes in the topsoil layers.

Key words: water tracing; water balance model; chloride; uncertainty; input–output budget; forest ecosystem; preferential flow; nutrient leaching; soil; hydrology.

Received 12 February 2018; accepted 29 July 2018;
published online 4 September 2018

Electronic supplementary material: The online version of this article (https://doi.org/10.1007/s10021-018-0295-4) contains supplementary material, which is available to authorized users.

Author contributions: GvdH developed and applied the hydrological model and the uncertainty analysis procedure, interpreted the data, wrote and edited the manuscript. AH contributed to the application of the hydrological model to experimental data. SD, CN set up the experimental design of the Fougères experimental forest, collected and analyzed the field samples over the monitoring period. ED, AL set up the experimental design of the chloride tracing experiment, contributed to the development and application of the hydrological modeland uncertainty analysis to the field data and edited the manuscript.

**Corresponding author; e-mail:* gregory.van-der-heijden@inra.fr

Introduction

In numerous forest ecosystems throughout Europe and North America, elevated atmospheric inputs of anthropogenic inorganic sulfur (SO_4^{2-}) and nitrogen (NH_4^+ and NO_3^-) over the past century have

contributed to the acidification of forest soils and surface waters. If not immobilized in the soil or plants, sulfate and nitrate inputs are leached below the rooting zone accompanied by cations such as magnesium, calcium, potassium and aluminum species (Reuss and Johnson 1986). Atmospheric inputs of inorganic sulfur have strongly decreased since the 1980s (Boxman and others 2008; Vuorenmaa and others 2017) but many studies have reported elevated pools of exchangeable sulfate in the soil (adsorbed during the period of elevated inputs) which, as they slowly desorb, sustain the sulfate leaching flux in the soil (Hodson and Langan 1999; van der Heijden and others 2011; Vuorenmaa and others 2017). Additionally, inputs of inorganic nitrogen have not systematically decreased (Vuorenmaa 2004; Cooper 2005). Consequently, an on-going depletion of exchangeable nutrient cations (Mg, Ca and K) in the soil due to elevated nutrient leaching fluxes has been reported in many forest ecosystems (Huntington and others 2000; Boxman and others 2008; Bedison and Johnson 2010; van der Heijden and others 2011; Jonard and others 2012) and has been, in some cases, related to a degradation of tree nutrition (Jonard and others 2015; Court and others 2018). The estimation of nutrient leaching fluxes is therefore an important stake for forest ecosystem sustainability. The leaching flux is a major component of input–output budgets (Ranger and Turpault 1999), which are used to assess changes in bioavailable pools of nutrients in the soil over periods of time ranging from several years to several decades and support forest management and policy decision making (for example, Norton and Young 1976; Johnson and Todd 1998; Dambrine and others 2000; Sverdrup and others 2006; Akelsson and others 2007; Johnson and others 2008; Jonard and others 2012).

As the direct measurement of the draining flux of water and nutrients is almost impossible in forest ecosystems (Bormann and Likens 1967), nutrient leaching in the soil profile and below the rooting zone is commonly estimated by coupling the nutrient concentrations measured in the soil water to the water flux simulated with a hydrological model. Hydrological models are also useful tools to predict the availability of water for plant uptake in the soil which directly impacts forest growth (Bréda and others 2006; Kirchen and others 2017) and may also impact nutrient bioavailability (Giesler and others 1996; Marques and others 1996; Weihermuller and others 2007). Many different hydrological models exist (for example, Granier and others 1999; Ogee and others 2003; Simunek and others 2003; Christiansen and others 2006; Neitsch and others 2011), varying in their complexity of the representation of water flow mechanisms, and compute the change in water content and water fluxes in the soil profile from input data (precipitation, potential evapotranspiration, and so on) and model parameters (soil hydrological properties, tree and canopy properties, etc.). At the soil profile scale, measured soil moisture datasets are most commonly used to calibrate and validate the hydrological model at each studied site (Granier and others 1999; Gérard and others 2004). However, when no soil moisture dataset was available, other datasets have been used for model calibration: measured natural variations of chloride concentration in soil solution (Legout and others 2016; Yu and others 2016), experimental water tracing data (van der Heijden and others 2013). Because the different datasets do not represent the same processes, modeling results are likely to depend on the subjective choice or availability of observational data used to calibrate hydrological models at the soil profile scale. For instance, experimental water tracing data are probably the most adequate data to demonstrate the occurrence of preferential water flow in the soil profile and are thus probably the best calibration dataset choice to model matrix and preferential water flow. Recent studies of the biological cycle of chloride (plants and soil micro-organisms) in forest ecosystems question the non-reactive transport of chloride in the soil (Öberg and others 2005; Svensson and others 2012; Montelius and others 2015) and thus question calibrating the model with natural variations of chloride concentration in soil solution.

The knowledge and quantification of model uncertainties is essential to compare different calibration methods (fitted model parameters and simulated model outputs). Uncertainty assessment of model simulations is also essential when models are used to support ecosystem management decisions and policies (Beven 1989). Hydrological model uncertainties have been addressed by various regression and probabilistic approaches: Generalized Likelihood Uncertainty Estimation (GLUE) (Beven and Binley 1992), Markov Chain Monte-Carlo (MCMC) (Kuczera and Parent 1998) or Bayesian inference approaches (Kavetski and others 2006). The GLUE procedure is a relatively simple and efficient optimization approach, is easy to implement into the code of existing models, does not require elevated computational costs (Zheng and Keller 2007; Yang and others 2008; Shen and others 2012; Rivera and others 2015), and is commonly used in hydrological modeling (Beven and

Binley 2014). It is ''based upon making a large number of runs of a given model with different sets of parameter values, chosen randomly from specified parameter distributions. On a basis of comparing predicted and observed responses, each set of parameter values is assigned a likelihood of being a simulator of the system.'' (Beven and Binley 1992). The majority of the applications of the GLUE approach to date have been in rainfall-runoff modeling. To our knowledge, no studies has yet quantified the uncertainties associated with drainage water fluxes and nutrient leaching fluxes at the soil profile scale in forest ecosystems.

The objective of this study was to compare three calibration methods of a simple daily water balance model, each using a different dataset (daily soil moisture measurements, monthly measurements of chloride concentrations in soil solution, and the elution of a concentrated chloride tracer) and to evaluate the influence of the calibration method on model outputs and uncertainty. For the three calibration datasets mentioned above, we hypothesize that:

1. Calibrating with daily soil moisture data yields the best estimation of the distribution of water uptake and water drainage in the soil profile
2. Calibrating with experimental water tracing data yields the best model performance for matrix and preferential water flow partitioning
3. When soil moisture data are unavailable, calibrating with natural variations of chloride concentrations in soil solution yields a comparable and satisfactory estimation of the distribution of water uptake and water drainage in the soil profile

For this purpose, we developed a simple pool and flux daily water balance model (WatFor) the structure of which is analogous to most lumped parameter pool and flux water balance models. A procedure based upon the GLUE approach was developed and implemented in the WatFor model to quantify the uncertainty in model parameter estimations. Finally, a Monte-Carlo approach was applied to estimate the uncertainty in the modeled water drainage and nutrient leaching flux in the soil profile. We used the monitoring data (soil moisture and monthly measurements of chloride concentrations in soil solution datasets) (Legout and others 2009b) and the experimental chloride water tracing dataset (Legout and others 2009a) from the Fougères experimental forest in Brittany (France). Finally, a Monte-Carlo approach was applied to estimate the uncertainties in model outputs (water drainage and nutrient leaching fluxes).

Materials and Methods

Study Site

Site and Soil Description

The study was carried out in the state forest of Fougères located in Northeastern Brittany in France (48°23′4″ N; 1°8′10″ W). The climate is temperate oceanic with a mean annual precipitation of 868 mm and a mean annual temperature of 12.9°C for the 1996–2006 decade. Two experimental sites (0.48 ha each) named Fou3 and Fou30 and located in a flat, homogeneous forested area of 5 ha under 90-year-old beech (*Fagus sylvatica* L.) were used in this study. The bedrock is granite and the thickness of the weathered granite varies between 3 and 5 m (Van Vliet-Lanoë and others 1995). This saprolite is covered by about 1.5 m of carbonate poor eolian loess (Toutain 1965). Several authors have recorded the homogeneity of the Fougères forest soils, that is, the same soil type was identified for the whole of this area (Toutain 1965; Legout and others 2008). In 1996, two soil pits were opened near the experimental site and these soils were described, sampled by level (Tables 1, 2) and analyzed. The humus was classified as moder (Baize and Girard 1998), whereas the soils were classified as glossic Alocrisols–Néoluvisols (Baize and Girard 1998) or as glossalbic Cambisols (IUSS Working Group WRB 2007). Funnel-shaped glossic tongues, which are wider at the top, appear below depths of 55 cm and develop vertically down to the weathered granite.

Soil hydrological properties were measured from soil cylinders (98 cm^2) sampled at 10, 30, 67.5 and 120 cm depth in two soil pits (5 replicates per depth and per pit). The volumetric water content (θ) was measured at different water potentials (from pF = 0 to 4.2) using a Richards chamber (Table 2).

Ecosystem Monitoring: Data Collection

The monitoring equipment installed at the two study plots (Fou3 and Fou30) has been described in detail in two previous studies (Legout and others 2009a; b). Only a brief summary is given here. Daily weather data were collected at the RENECOFOR HET35 weather station (ICP Forests network) located in a clearing in the Fougères forest (48°22′ N; 1°10′ W): daily precipitation, air temperature and relative humidity, wind speed and direction and soil heat flux (station set up in Jan-

Table 1. Chemical Properties of the Soil at the Fougères Experimental Forest

Depth	pH_{water}		Soil carbon		Exchangeable pool											
					ECEC		Al		Mg		Ca		K		BS	
			g kg^{-1}		$cmol_c$ kg^{-1}		$cmol_c$ kg^{-1}		$cmol_c$ kg^{-1}		$cmol_c$ kg^{-1}		$cmol_c$ kg^{-1}		%	
0–10	3.94	*0.06*	44.64	*4.4*	5.88	*0.37*	5.32	*0.48*	0.25	*0.05*	0.36	*0.10*	0.22	*0.02*	14.4	*1.7*
10–20	4.34	*0.04*	16.16	*1.7*	3.32	*0.26*	3.03	*0.41*	0.06	*0.01*	0.11	*0.04*	0.09	*0.01*	10.2	*2.8*
20–30	4.4	*0.03*	10.94	*1.2*	2.58	*0.19*	2.24	*0.33*	0.03	*0.01*	0.07	*0.02*	0.08	*0.01*	10.5	*2.3*
30–40	4.4	*0.03*	7.1	*1.4*	2.10	*0.20*	1.85	*0.39*	0.02	*0.01*	0.07	*0.03*	0.07	*0.01*	11.0	*2.0*
40–50	4.4	*0.02*	5.05	*0.8*	2.80	*0.35*	2.64	*0.46*	0.04	*0.01*	0.06	*0.02*	0.09	*0.01*	11.4	*3.5*
50–60	4.4	*0.03*	3	*0.8*	3.50	*0.74*	3.43	*0.85*	0.05	*0.01*	0.05	*0.00*	0.10	*0.02*	11.7	*6.6*
60–70	4.4	*0.02*	2.35	*0.4*	4.65	*0.45*	4.24	*0.51*	0.13	*0.06*	0.07	*0.02*	0.13	*0.01*	10.5	*3.7*
70–80	4.4	*0.03*	1.7	*0.2*	5.80	*0.59*	5.04	*0.50*	0.21	*0.11*	0.08	*0.04*	0.15	*0.02*	9.3	*2.3*
80 -90	4.5	*0.03*	1.5	*0.1*	6.20	*0.37*	5.17	*0.33*	0.41	*0.14*	0.11	*0.05*	0.16	*0.01*	12.8	*2.7*
90–100	4.6	*0.05*	1.3	*0.2*	6.60	*0.41*	5.30	*0.44*	0.60	*0.27*	0.14	*0.08*	0.16	*0.01*	16.3	*5.0*
100–110	4.7	*0.04*	1.35	*0.1*	6.55	*0.29*	4.92	*0.35*	0.72	*0.25*	0.16	*0.07*	0.16	*0.01*	17.8	*4.7*
110–120	4.8	*0.06*	1.4	*0.2*	6.50	*0.41*	4.54	*0.54*	0.84	*0.43*	0.17	*0.11*	0.15	*0.01*	19.3	*7.9*

Values in italic font represent the standard deviation.

uary 1997). Daily potential evapotranspiration (PET) was calculated with the Penmann formula.

In the Fou3 plot, four soil pits (7 m long and 1 m wide) were opened in 1996 and rapidly equipped with Time Domain Reflectometry (TDR) probes (TRIME-TDR Imko1), ceramic cup tension lysimeters (0.5 m long) and zero tension plate lysimeters (0.4 × 0.3 m). TDR probes, tension ceramic cup lysimeters (TCL and zero tension plate lysimeters (ZTL) were inserted horizontally into the soil at 10, 30, 55, 80 and 120 cm depth in the undisturbed soil. After connecting the systems, the pits were closed, replacing the soil layers in their correct order. In total, four replicates per depth of TCL and ZTL (except for 80 and 120 cm depth where only two replicates of ZTL were installed) and one replicate per depth of TDR probes were installed. In December 1999, Fou3 was badly damaged by storm Lothar (Legout and others 2009b): 60% of standing trees were uprooted and 30% had their trunk snapped. The Fou30 plot was set up in 2000 close to the Fou3 plot, in the same forest management plot but in an area that was not damaged by the Lothar storm. Two replicates of TDR probes were installed at 10, 30, 55, 80 and 120 cm depth. Four replicates of zero tension lysimeters were installed at 0 cm (just below the humus layer), 10 cm and 30 cm depth. Eight replicates of ceramic tension-cup lysimeters were installed at 10 and 30 cm depth and 16 replicates were installed at 55, 80 and 120 cm depth to capture the spatial variability due to the presence of glossic structures.

Over the 1999–2004 monitoring period, soil solution samples were collected from each lysimeter every 28 days per depth. Before analysis, samples collected with ceramic cups were bulked to obtain four composite samples per depth (one for each side of the pit). Samples collected by zero tension lysimeters were bulked to obtain 1 composite sample per depth. The samples collected with zero tension lysimeters were filtered rapidly in the laboratory through a 0.45 mm Metriciel Membrane Filter and stored in the dark at 2°C while waiting for analysis. The ceramic cup solutions were not filtered, the pore size of the ceramic being 0.45 mm. Cl^- and NO_3^- concentrations in samples were analyzed by colorimetric methods (Traacs 2000, Bran and Luebbe) and Ca concentrations were measured by ICP-AES (Inductively Coupled Plasma-Atomic Emission Spectrometry; JY 180 Ultrace, Jobin–Yvon).

Soil Water Tracing Experimental Design

In March 2006, in the Fou30 plot, 31 mm of a chloride-enriched solution (616 mg l^{-1}) were applied to an experimental plot that encompassed the instrumented areas. The water used was pumped from a forest stream located near the site, stored in a large plastic tanker and NaCl, $CaCl_2$ and $MgCl_2$ were added to the tanker to obtain a 616 mg l^{-1} chloride solution. The enriched solution was sprinkled onto the soil using an oscillating ramp to simulate precipitation under the canopy. To obtain a homogeneous application and to avoid border effects, the simulated precipitation was applied to two plots (6 × 11 m) surrounding each pit. The tracer application on March , 2006 was followed by three simulated rain applications (stream water

Table 2. Physical Properties of the Soil at the Fougères Experimental Forest

Depth	Bulk density		Granulometry								Hydrological properties			
			Clay		Fine silt		Coarse silt		Fine Sand		Coarse sand			
	g cm^{-1}		g kg^{-1}		g kg^{-1}		g kg^{-1}		g kg^{-1}		g kg^{-1}			
0–10	0.908	*0.06*	165.4	*6.4*	248.8	*4.4*	476.2	*5.6*	99	*6.3*	11	*2.1*	$\theta_{pF=4.2}$ %	19.8 *5.6*
10–20	1.132	*0.03*	145.4	*6.6*	246	*4.0*	489.4	*5.7*	107.4	*10.1*	11	*3.9*		18.3 *3.0*
20–30	1.172	*0.02*	137	*5.5*	245	*4.1*	493.4	*4.8*	113	*8.8*	11	*3.5*		18.3 *3.0*
30–40	1.22	*0.03*	128	*7.1*	245	*6.8*	497	*6.2*	119	*12.9*	11	*5.0*		19.0 *2.5*
40–50	1.32	*0.02*	142.5	*8.3*	239.5	*4.8*	489.5	*5.2*	119	*9.3*	9.5	*3.3*		19.4 *2.7*
50–60	1.42	*0.02*	157	*15.5*	234	*6.9*	482	*8.6*	119	*13.1*	8	*4.2*		19.9 *3.3*
60–70	1.455	*0.02*	178	*10.3*	228	*5.8*	481	*8.3*	104.5	*11.1*	8	*2.5*		20.4 *4.3*
70–80	1.49	*0.03*	199	*14.3*	222	*9.9*	480	*13.8*	90	*18.3*	8	*3.0*		20.4 *4.3*
80 -90	1.515	*0.02*	208	*8.5*	232.5	*8.3*	466	*14.2*	79	*10.7*	14.5	*5.7*		21.8 *2.0*
90–100	1.54	*0.03*	217	*10.2*	243	*13.2*	452	*24.6*	68	*12.0*	21	*10.7*		21.8 *2.0*
100–110	1.575	*0.02*	214	*6.5*	250	*10.9*	425.5	*20.7*	69.5	*7.2*	41	*15.3*		21.8 *2.0*
110–120	1.61	*0.02*	211	*7.9*	257	*16.8*	399	*34.0*	71	*9.1*	61	*27.5*		21.8 *2.0*

													$\theta_{pF=1.5}$ %	39.5 *1.7*
														39.1 *1.6*
														38.8 *1.8*
														38.3 *2.2*
														38.3 *2.2*
														35.8 *0.7*
														35.8 *0.7*
														35.8 *0.7*
														35.8 *0.7*

													$\theta_{pF=0}$ %	53.1 *3.5*
														49.0 *2.1*
														49.0 *2.1*
														47.3 *1.6*
														46.1 *1.6*
														44.9 *1.7*
														43.4 *2.2*
														43.4 *2.2*
														40.9 *1.2*
														40.9 *1.2*
														40.9 *1.2*
														40.9 *1.2*

Values in italic font represent the standard deviation.

without chloride enrichment) on March 9 (16.8 mm), March 10 (15.3 mm) and lastly on March 14, 2006 (14.9 mm). The average rainfall intensity for the tracer application was 4.4 mm h^{-1} and the three successive simulated rainfall events without chloride enrichment were, respectively, 5.6, 5.1 and 2.5 m h^{-1}.

After the tracer application, soil solution samples from each lysimeter were collected individually. During the first week, the sampling frequency varied from 6 to 24 h, but then decreased gradually to reach 1 month at the end of the experiment (September 1, 2007). In the laboratory, zero tension lysimeter samples were filtered through 0.45 µm Metriciel membrane filters. All the samples were stored in the dark at 2°C and chloride was analyzed rapidly by colorimetry (Traacs 2000, Bran et Luebbe). The quantification limit of this method was 0.2 mg l^{-1}. The precision of this method is less than 5% and control standards were systematically measured during sample sequences for quality control. For the water tracer experiment, individual samples were not bulked together for analysis.

The monitoring of the elution of the enriched chloride tracer solution in the soil profile evidenced preferential flow paths (Legout and others 2009a) and showed that around 17% of the applied tracer mass transited in the soil via these preferential flow paths.

WatFor Hydrological Model Description

WatFor is a daily water balance model composed of two modules that, respectively, compute the fluxes of water and a non-reactive solute such as chloride in forest ecosystems (van der Heijden and others 2013; Legout and others 2016; van der Heijden and others 2017). WatFor accounts for canopy rainfall interception, throughfall, soil water content change and water drainage in the soil profile. The hydrological module of WatFor was inspired from the structure of the BILJOU water balance model (Granier and others 1999). A description of the hydrological module of the WatFor model is given in Figure 1. The non-reactive solute transport module was inspired from a previous model which was developed to simulated the transport of deuterium tracer applied on the forest floor (van der Heijden and others 2013). The model inputs are daily rainfall and daily potential evapotranspiration. The soil profile is divided into different layers (user-defined) and for each layer, the following parameters are required: layer thickness, bulk density (kg m^{-3}), fraction of stones (> 2 mm) (no unit), water uptake distribution parameter in the

layer (fraction of total water uptake), volumetric water content ($m^3\ m^{-3}$) at wilting point (θ_{WP}), field capacity (θ_{FC}) and saturation (θ_{Sat}).

Precipitation interception was calculated using a simplified version of the interception model proposed by Aussenac (1968) and used in the BILJOU model. If the daily rainfall is below the fitted threshold (In_{thresh}), the canopy intercepts 100% of rainfall. If the daily rainfall exceeds In_{thresh}, interception is calculated as a linear function of rainfall (Figure 1) where the slope (a) of the linear model is fitted and the intercept (b) is computed from the value of the In_{thresh} parameter as follows:

$$In(t) = a \times RF(t) + b \quad (1)$$

$$b = In_{thresh} \times (1 - a) \quad (2)$$

where, $In(t)$ is the canopy rainfall interception ($L\ m^{-2}\ day^{-1}$) at time step t, and $RF(t)$ is the daily rainfall ($L\ m^{-2}\ day^{-1}$) at time step t. Although this interception model does not allow for canopy saturation, it is a simple model requiring few parameters; it accounts for the evaporation of intercepted water between rainfall events occurring the same day; and it has been proven to successfully reproduce canopy interception for different tree species (Legout and others 2016).

The daily evapotranspiration flux (T) from each soil layer is computed from the daily potential evapotranspiration and the water uptake distribution parameter in each soil layer. The model allows changes in the water uptake profile when the soil water content becomes limiting for water uptake. When the relative extractable water (soil water between field capacity and wilting point) is below 0.4, the potential evapotranspiration flux from the given soil layer is reduced (Granier and others 1999). When the actual water uptake in the soil layer is below of the layer potential evapotranspiration, the difference between potential and actual evapotranspiration is transferred to the soil layer directly below.

Water fluxes in the soil Each soil layer is divided into two types of water flow: preferential flow (macropores) and matric flow (micropores). The daily throughfall flux is divided into two components (preferential and matric flow) as a function of throughfall intensity and the moisture content of the topsoil layer (Figure 1). When the throughfall flux is below the preferential flow threshold model parameter (representing the infiltration capacity in $mm\ day^{-1}$ of the topsoil layer), 100% of the throughfall flux is directed into the micropores. When the throughfall flux exceeds this threshold, a flux of water equal to the threshold is directed into the micropores and the remaining throughfall flux is directed into the macropores. The value of the preferential flow threshold model parameter varies with the soil moisture content of the topsoil layer. Preferential flow threshold parameters for the field capacity and wilting point soil moistures are fitted during the calibration process. The preferential flow threshold is then linearly interpolated at each time step.

Water flows vertically in the soil profile as both matric and preferential flow. In the micropores, matric flow between two soil layers is generated when the soil moisture exceeds the field capacity moisture (θ_{FC}). In the macropores, water is not bound to the soil and flows to the macropores of the layer directly below. In each soil layer, depending on the micropores soil water content, a fraction of the preferential water flux is redirected to the micropores as follows:

$$Q_{PF \rightarrow M}(t) = [W_{FC} - W(t)] \times PF_2M \quad (3)$$

where, $Q_{PF \rightarrow M}(t)$ is the flux of water from the macropores toward the micropores (mm) at time step t, W_{FC} is the soil water content at field capacity (mm), $W(t)$ is the soil water content at time step t (mm), and PF_2M is a user-defined model parameter comprised between 0 and 1 (unitless). Finally, matric water flow occurs when the soil water content of the soil layer exceeds field capacity.

Non-reactive transport of chloride Model inputs are composed of monthly atmospheric inputs of Cl: Cl concentrations in rainfall and Cl dry deposition. Dry deposition was calculated from the bulk precipitation and throughfall monitoring data assuming no canopy exchange (Adriaenssens and others 2013). In the model, the input flux of Cl from rainfall and dry deposition are mixed to form the Cl throughfall flux (concentrations in throughfall are corrected for canopy interception). The throughfall flux of Cl is then divided into the macro- and micropores according to the preferential flow generation formula described above. In the soil, Cl concentrations are computed from the mixing of the different water pools and fluxes. WatFor assumes no Cl uptake by plants, soil macro or micro biota and no interactions with soil particles (for example, surface adsorption).

WatFor Parameter Optimization Procedure

A numerical optimization procedure based on the Generalized Likelihood Uncertainty Estimation (GLUE) approach was developed to (1) estimate

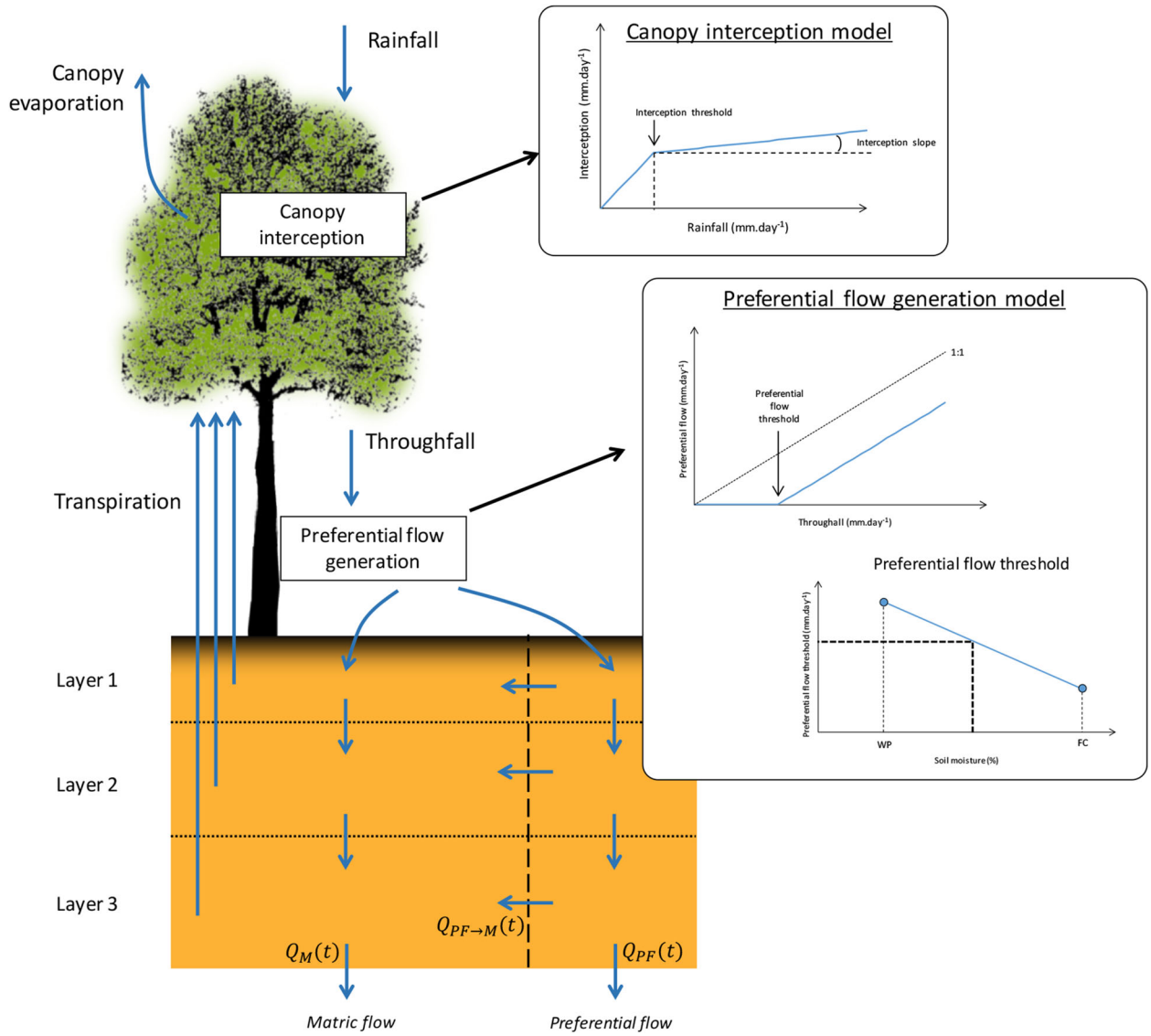

Figure 1. Depiction of the WatFor forest hydrological model.

model parameters for which the best fit between modeled and measured datasets is obtained, and (2) quantify uncertainties associated with parameter estimations. This procedure is ''based upon making a large number of runs of a given model with different sets parameter values, chosen randomly from specified parameter distributions. On a basis of comparing predicted and observed responses, each set of parameter values is assigned a likelihood of being a simulator of the system.'' (Beven and Binley 1992).

This procedure was applied to simultaneously estimate the preferential flow generation parameters, and, for each soil layer, the root distribution and PF_2M parameters. To limit the number of parameters to estimate, the parameters were optimized for the following soil layers: 0–20 cm, 20–40 cm, 40–60 cm, 60–100 cm and 100–120 cm (that is, model parameters were assumed to be equal between for the 0–10 cm and 10–20 cm layers, for example). These layers were selected following the distribution of TDR probes and lysimeters in the soil. The different steps of the procedure are summarized in Figure 2. The optimization procedure was applied to the three calibration datasets independently: daily soil moisture measurements (noted θ optimization), monthly measurements of chloride concentrations in TCL solutions ($[Cl]_{Nat}$ optimization), and the elution of a concentrated chloride ($[Cl]_{Tracer}$).

First, the boundaries (minimum and maximum) for each parameter were set (Figure 2-1). For the

water uptake distribution and PF_2M factors in each soil layer, the minimum and maximum parameter values were set to 0 and 100%. The minimum and maximum preferential flow generation parameters (both field capacity and wilting point) were set to 0 and 30 mm day^{-1}. Then, a set of parameters is randomly selected (Figure 2-2) within these boundaries (random selection following an even distribution). The WatFor is then run over the dataset period (1999–2004 for the θ and $[Cl]_{Nat}$ datasets and 2006–2007 for the $[Cl]_{Tracer}$ dataset) (Figure 2-3). From the modeled data, indicators of the goodness of fit between modeled and measured data are computed (Figure 2-4). For the $[Cl]_{Nat}$ and $[Cl]_{Tracer}$ datasets, the mean absolute error (*i.e.*, absolute difference between the modeled and measured monthly chloride concentrations) was used as the goodness of fit indicator. The mean absolute error was calculated for each TCL depth (10, 30, 55, 80 and 120 cm). For the θ dataset, given the cycling nature of the dataset, the mean absolute error indicator was not efficient enough to discriminate the best model runs. Instead we used an indicator counting the number of days for which the modeled soil moisture was within ± 10% of the measured soil moisture. This count indicator was also calculated for each TDR depth (10, 30, 55, 80 and 120 cm). The scores of each goodness of fit indicator and the associated model parameters are stored (Figure 2-5) and a new set of randomly selected parameters is generated (Figure 2-2). This cycle was replicated n times. After the last replicate, the stored parameters are ranked according to each of the five indicators. If a parameter set yielded an indicator below (for the TDR dataset) or above (for the ''Nat Chloride'' and ''Tracer Chloride'' datasets) a user-defined quantile level (p), the parameter set was rejected (Figure 2-6). From the remaining population of parameters, new parameter boundaries are defined (Figure 2-7) and the cycle is repeated (N iterations). The modeled parameter boundaries after 10 iterations are used to estimate the range of optimal model parameters and quantify their associated uncertainty. The repeatability of estimated parameter boundaries was estimated by repeating the whole procedure five times and

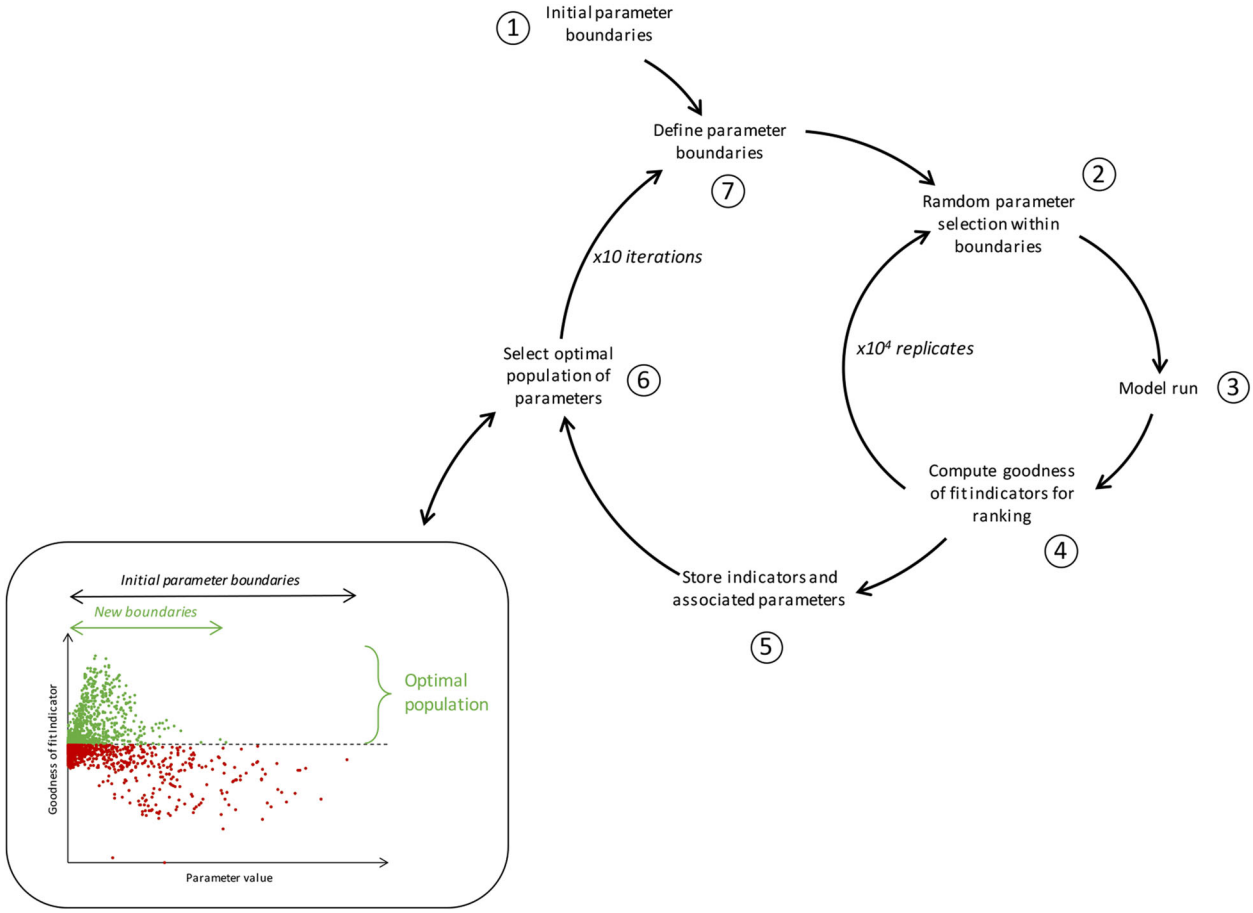

Figure 2. Description of the Generalized Likelihood Uncertainty Estimation optimization procedure.

calculating the standard deviation for each parameter boundary.

Different values for the optimization procedure parameters (N, n and p) were tested (Figure S1). These tests showed that, for n values below $2.5{\cdot}10^3$, the optimization procedure converged toward narrow ranges (Figure S1-A) but the repeatability of this convergence was poor (data not shown). For n values above $5.0{\cdot}10^3$, the convergence was similar but the convergence was more repeatable when n was set to 10^4. The quantile level parameter p was rather sensitive (Figure S1-B). For values equal or above to 60%, the optimization procedure converged toward narrow but poorly repeatable ranges. For values below 50% the convergence of the procedure over 10 iterations was unsatisfactory. For these reasons, the optimization procedure parameters were set at 10^4 replicates per iteration and a quantile level of 50%. Convergence and repeatability with these two parameters is shown in (Figure S1-C). Five estimates of parameter boundaries were obtained from five different optimization procedure runs to monitor repeatability. Parameter boundaries presented in this study are the average value of these five replicates.

The three optimization strategies were compared using different indicators. Firstly, the performance of the optimization procedure was assessed using the model parameter convergence and the repeatability of the convergence described previously. Secondly, the performance of each strategy at reproducing the three datasets (daily soil moisture, monthly chloride concentrations and chloride tracing experiment) was assessed visually and by calculating the mean and root means square error between the modeled and measured datasets. Finally, model outputs (water drainage, nutrient leaching and their associated uncertainties) were compared between strategies.

Water Drainage Flux and Nutrient Leaching Flux Uncertainty

The uncertainty in the water drainage fluxes was estimated by applying a Monte-Carlo modeling approach. First, model parameters were randomly selected within their uncertainty range estimated by the GLUE modeling approach described above. Then the model was run over the 1999–2005 period to compute the daily water drainage flux. The nutrient leaching flux was calculated as the product of the monthly water drainage flux (matric + preferential flow) and measured TCL solute (Ca, NO_3 and Cl) concentrations at the corresponding depth (solute concentrations were randomly selected from a normal distribution defined from the monthly average and standard deviation concentration). This procedure was iterated 10^4 times and the standard deviation of the 10^4 replicated water drainage and nutrient fluxes were computed on a monthly and yearly time scale.

To test the influence of water type selection on modeled results, the Monte-Carlo was applied a second time to the ''Nat Chloride'' calibration dataset. The nutrient leaching flux was decomposed into a matric component (product of the monthly water matric drainage flux and measured TCL solute concentrations) and a preferential component (product of the monthly water preferential drainage flux and measured ZTL solute concentrations).

Results

Model Parameter Estimates

The lowest uncertainty for water uptake distribution parameter in each soil layer (Table 3) was obtained with the $[Cl]_{Tracer}$ strategy followed by the θ strategy and the $[Cl]_{Nat}$ strategy. The repeatability of the optimization procedure was best for the θ strategy (standard deviations) and poorest for the $[Cl]_{Tracer}$ strategy. The predicted ranges by all three strategies were in general agreement with one another. However, the water uptake distribution was slightly lower in the 0–20 cm layer and slightly higher in the 40–60 cm layer for the $[Cl]_{Tracer}$ strategy. The preferential flow parameter uncertainty was highest (infiltration capacity at the wilting point and field capacity) for the θ optimization. For the $[Cl]_{Nat}$ strategy, only the infiltration capacity at field capacity parameter converged to values between 5.7 and 8.8 mm day^{-1}. The $[Cl]_{Tracer}$ strategy was the most efficient to estimate preferential flow parameters. The infiltration capacity at field capacity converged to values between 6.6 and 6.9 mm day^{-1} and the infiltration capacity at wilting point converged to values between 15.0 and 25.9 mm day^{-1}. For the PF_2M parameter (water flux from macro to micropores), none of the three strategies converged satisfactorily. ϵ for these parameters were above 94% for the θ strategy, above 51% for $[Cl]_{Nat}$ and above 41% for $[Cl]_{Tracer}$.

Simulation of the Measured Datasets

Daily soil moisture dataset For all three optimization strategies, the range of variation of soil moisture between winter and summer periods was very

Table 3. Model Parameter Uncertainty Ranges Estimated with the GLUE Modeling Approach for the Three Optimization Strategies (''Soil Moisture,'' ''Natural Chloride'' and ''Tracer Chloride'') Expressed as Lower and Upper Boundaries

		Unit	Soil moisture				Natural chloride				Tracer chloride			
			Lower		Upper	ϵ	Lower		Upper	ϵ	Lower		Upper	ϵ
Root distribution	0–20 cm	%	51.7	*0.63*	71.5	*0.84*	19.8	55.1	*3.54*	82.5	*2.76*	27.4	42.7	*5.15*	49.7	*4.57*	7.0
	20–40 cm	%	2.2	*0.20*	21.2	*0.81*	19.0	4.4	*2.16*	33.9	*1.99*	29.6	2.1	*0.64*	7.5	*1.46*	5.3
	40–60 cm	%	14.1	*0.47*	24.9	*0.42*	10.8	1.1	*0.65*	16.6	*1.75*	15.5	29.3	*3.22*	39.2	*0.77*	9.9
	60–100 cm	%	0.4	*0.06*	14.2	*0.59*	13.8	0.2	*0.11*	11.1	*2.79*	10.8	4.5	*3.02*	15.4	*4.42*	10.9
	100–120 cm	%	1.8	*0.04*	3.2	*0.05*	1.5	0.2	*0.07*	2.3	*0.81*	2.1	3.5	*1.94*	7.1	*1.22*	3.6
PF parameters	Infilt_WP	mm day^{-1}	0.8	*0.21*	29.1	*0.35*	28.4	3.9	*1.10*	27.5	*0.59*	23.6	15.0	*4.22*	25.9	*1.07*	10.9
	Infilt_FC	mm day^{-1}	3.7	*0.12*	28.7	*0.39*	25.0	5.7	*0.35*	8.8	*0.32*	3.1	6.6	*0.18*	6.9	*0.23*	0.3
PF_2M factor	0–20 cm	%	2.4	*1.15*	96.8	*0.97*	94.4	2.7	*1.53*	54.3	*12.01*	51.6	29.8	*11.58*	81.5	*10.85*	51.6
	20–40 cm	%	2.0	*0.68*	97.1	*1.15*	95.1	17.6	*5.06*	88.4	*5.81*	70.8	36.7	*3.65*	78.3	*13.09*	41.6
	40–60 cm	%	2.9	*0.73*	97.6	*0.79*	94.7	8.8	*2.70*	84.6	*5.92*	75.8	11.4	*6.56*	56.1	*22.91*	44.8
	60–100 cm	%	3.4	*0.89*	97.7	*0.99*	94.4	9.3	*3.80*	90.1	*4.45*	80.7	32.8	*14.54*	81.1	*4.47*	48.3
	100–120 cm	%	2.9	*1.26*	97.7	*1.05*	94.8	12.5	*6.27*	92.4	*1.44*	79.9	39.1	*20.74*	80.4	*6.74*	41.3

Values in italic font represent the standard deviation of upper and lower boundaries over the 5 optimization replicates, ϵ is the difference between the upper and the lower boundary.

similar between measured and modeled datasets (Figure 3). Over the entire period modeled soil moisture values were mostly within measurement uncertainty. Certain hydrological events during the vegetation period were not accurately reproduced in amplitude but the dynamics of drying and wetting were reproduced. In general, the modeled rewetting of soil porosity was faster compared to the measured data. The differences in root mean square error between modeled and measured soil moisture (Table 4) for the three optimization strategies were small but show that soil drying and wetting dynamics were best reproduced by the soil moisture optimization strategy.

In the topsoil (10 cm depth), uncertainty was slightly lower for the $[Cl]_{Tracer}$ strategy (average: 0.3%; maximum: 3.4%) compared to the θ (0.5%; maximum: 4.1%) and $[Cl]_{Nat}$ (0.6%; maximum: 4.9%) strategies. For the deeper soil layers, uncertainty in soil moisture predictions was very similar between all three optimization strategies except at 120 cm depth where the $[Cl]_{Tracer}$ strategy uncertainty was higher (average 0.8%; maximum: 5.4%) compared to the θ (0.5%; maximum: 4.0%) and the $[Cl]_{Nat}$ (0.6%; maximum: 4.3%) strategies.

Natural variations of chloride concentrations The slight increasing trend observed in the monitoring of natural chloride concentrations in soil solution at 10 and 80 cm depth was reproduced by the WatFor model for all three optimization strategies (Figure 4). Seasonal variations of chloride concentrations were not accurately reproduced but the concentration levels and the range of seasonal variation were reproduced. Similarly to uncertainties in soil moisture predictions, the uncertainty in natural chloride concentration predictions was lower for the $[Cl]_{Tracer}$ strategy in the topsoil: average 5.4 µmol l^{-1} and maximum 25. 2 µmol l^{-1} at 10 cm depth compared to 13.1 and 17.9 µmol l^{-1} (average) and 71.3 and 97.1 µmol l^{-1} (maximum), respectively, for the θ and the $[Cl]_{Nat}$ strategies. At 55, 80 and 120 cm depth, model uncertainties were very similar between the three optimization strategies.

Chloride tracer experiment The WatFor model was also able to correctly reproduce the general elution peak trends for all three optimization strategies (Figure 5). The spatial variability of measured chloride concentrations was high, especially in depth (spatial variability of water flow velocity) but an elution peak was observed in all individual lysimeters (Legout and others 2009a). The best fit was obtained for the $[Cl]_{Tracer}$ strategy. At 10 and 30 cm depth (data not shown), the modeled elution peak occurred at

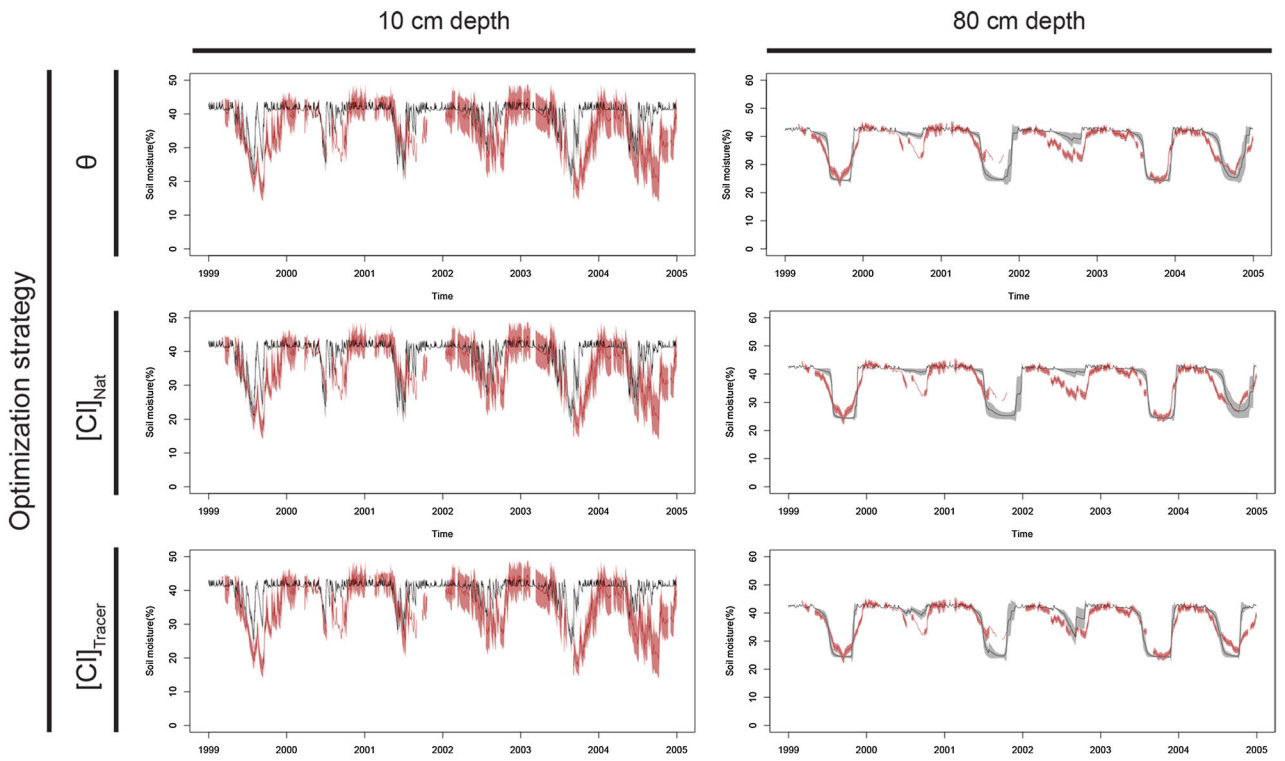

Figure 3. Modeled (black line) and measured (red line) daily volumetric soil moisture variations (%) at 10 and 80 cm depth for the three optimization strategies (θ, $[Cl]_{Nat}$ and $[Cl]_{Tracer}$) over the 1999–2004 period. The gray and red area around the lines represents the uncertainty in modeled and measured data (Color figure online).

Table 4. Mean Error and Root Mean Square Error Between the Measured and Modeled Data (Daily Soil Moisture, Monthly Natural Chloride Concentrations and Water Tracing Experiment Chloride Concentrations) for the Three Optimization Strategies

Optimization	Dataset					
	Daily soil moisture		Monthly natural [Cl]		Tracing exp. [Cl]	
	ME (%)	RMSE (%)	ME (μmol l^{-1})	RMSE (μmol l^{-1})	ME (μmol l^{-1})	RMSE (μmol l^{-1})
θ	4.5	7.4	− 27.5	119.6	714	1777
	1.8	4.9	68.6	153.0	740	1703
	1.1	3.8	83.6	143.5	− 225	536
	1.1	3.5	59.5	145.6	− 273	482
	0.6	2.2	41.8	80.8	− 114	360
$[Cl]_{Nat}$	4.1	7.1	− 18.6	124.1	670	1508
	0.4	4.8	64.0	144.9	406	1482
	1.8	4.1	29.9	107.4	− 697	962
	1.2	3.7	29.9	129.1	− 295	380
	1.1	2.6	1.7	50.0	− 289	340
$[Cl]_{Tracer}$	5.2	7.9	− 50.1	115.6	566	1501
	3.9	5.9	4.9	107.7	85	949
	0.7	4.5	48.5	134.2	− 556	764
	0.8	3.3	12.8	114.1	− 292	373
	− 0.4	2.5	27.6	77.9	− 205	303

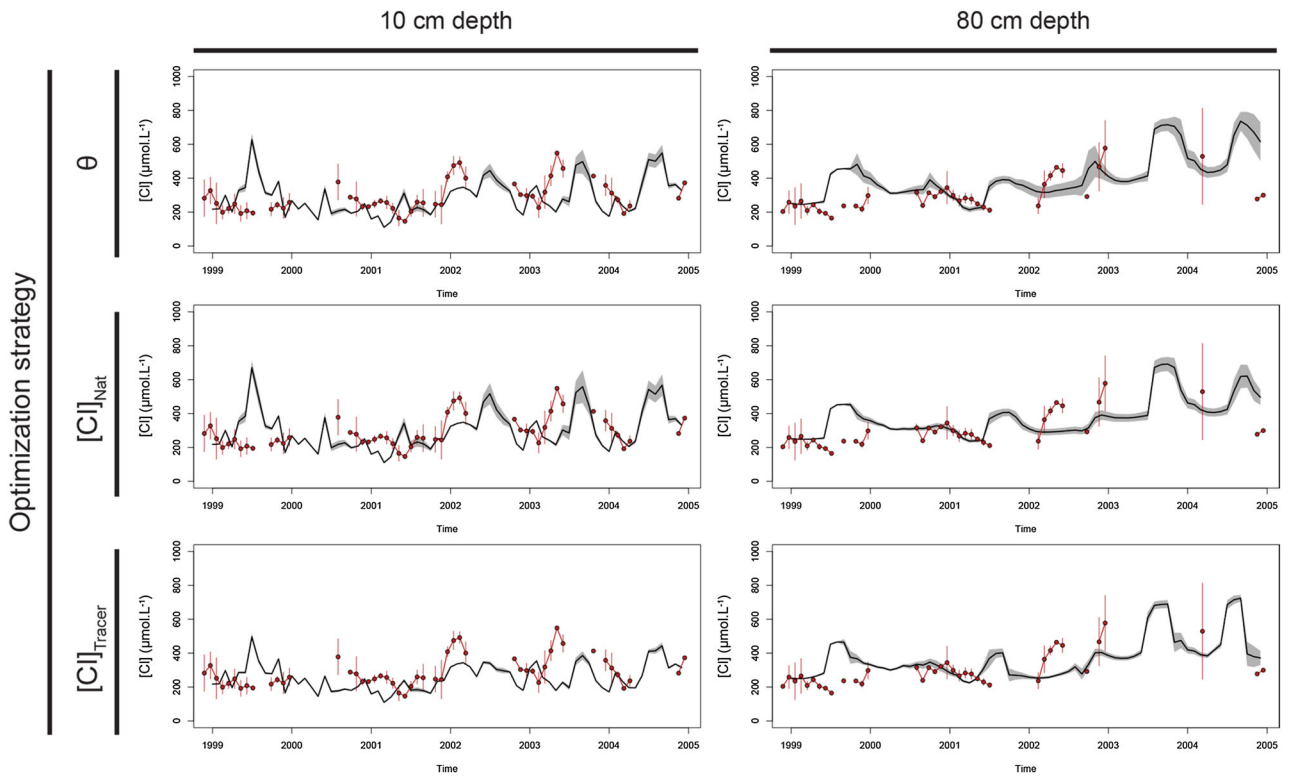

Figure 4. Modeled (black line) and measured (red line) natural chloride concentration variations (µmol l^{-1}) in tension-cup lysimeters solutions at 10 and 30 cm depth for the three model parameter optimization strategies (''Soil moisture,'' ''Natural chloride'' and ''Tracer chloride'') over the 1999–2004 period. The gray and red area around the lines represents the uncertainty in modeled and measured data (Color figure online).

the same for all three optimization strategies and was close to the measured elution peak but the amplitude of the elution peak exceeded the measured data. The modeled amplitude of the peak was greatest for the θ strategy and lowest for the $[Cl]_{Tracer}$ strategy. At depths below 55 cm, the amplitudes of the modeled elution peaks were much closer to the measured data. The θ optimization dataset differed from i) the other two strategies and ii) the measured data: modeled elution peaks occurred sooner. The $[Cl]_{Nat}$ strategy also reproduced very satisfactorily the tracing experiment data (Table 3). The percentage of modeled preferential flow with the $[Cl]_{Nat}$ strategy ranged from 16 to 39% over the 1999–2004 period, which was similar to the $[Cl]_{Tracer}$ strategy: 19–44%. Though differences between the $[Cl]_{Nat}$ and $[Cl]_{Tracer}$ strategies were small (Figure 5), the amplitude and occurrence of elution peaks at 80 and 120 cm (data not shown) were best reproduced by the $[Cl]_{Tracer}$ strategy. Finally, the modeled data (modeled chloride concentrations in micropores soil water) presented in Figure 5 does not enable one to observe the measured preferential flow elution peak that occurred in the first weeks after the application of the chloride tracer (Legout and others 2009a).

Model Outputs for the Different Optimization Strategies

Water Drainage Flux

The study period 1999–2004 covered years with variable weather conditions. The years 2003 and 2004 were very dry years and predicted water drainage in the soil profile was low (Table 5): from 144 ± 5 to 151 ± 4 mm $year^{-1}$ in 2003 at 120 cm depth. The year 2000 was the wettest year of the period: from 562 ± 7 to 564 ± 12 mm $year^{-1}$ in 2000 at 120 cm depth.

At all depths, the annual water drainage fluxes were lowest for the $[Cl]_{Nat}$ and highest for the $[Cl]_{Tracer}$ strategies (Table 5). Differences between optimization strategies were greater for the topsoil layers (10 and 30 cm depth): the maximum difference was 61.3 mm at 10 cm depth (2002) and 114.8 mm at 30 cm depth (2000). Differences between optimization strategies decreased with depth. At 80 and 120 cm depth, the predicted annual water drainage fluxes were very similar for

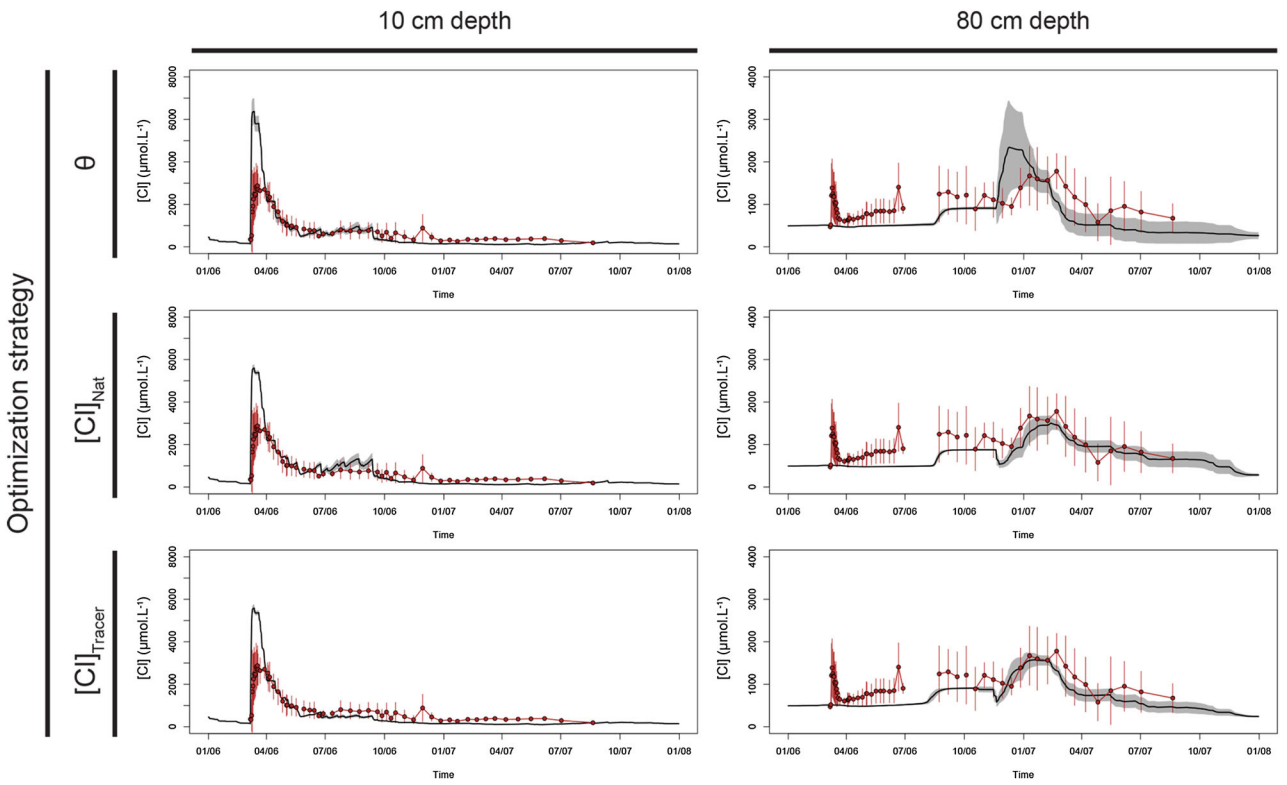

Figure 5. Modeled (black line) and measured (red line) elution of the chloride tracer (µmol l^{-1}) in tension-cup lysimeters solutions at 80 and 120 cm depth for the three model parameter optimization strategies (''Soil moisture,'' ''Natural chloride'' and ''Tracer chloride'') over the 2006–2007 period (Chloride tracer applied on March 8th 2006). The gray and red area around the lines represents the uncertainty in modeled and measured data (Color figure online).

the three different optimization strategies. The maximum difference was 36.3 mm at 80 cm depth (2004) and 30 mm at 120 cm depth (2004). The uncertainty in the modeled annual water drainage flux was very low (Table 5). Uncertainties were relatively similar at all depths and only slightly decreased with depth. At 30 cm depth, uncertainties ranged from 5.9 to 11.0 mm $year^{-1}$ for the θ strategy drainage fluxes, from 4.9 to 9.8 mm $year^{-1}$ for $[Cl]_{Nat}$, and from 4.2 to 8.4 mm $year^{-1}$ for $[Cl]_{Tracer}$. At 80 cm depth, uncertainties ranged from 4.8 to 11.7 mm $year^{-1}$ for the θ strategy drainage fluxes, from 3.6 to 6.5 mm $year^{-1}$ for $[Cl]_{Nat}$, and from 3.1 to 6.5 mm $year^{-1}$ for $[Cl]_{Tracer}$.

Nutrient Leaching Flux

No significant differences of annual nutrient leaching flux were observed between the three optimization strategies at 30 cm and 80 cm depth (Table 6). In general, $[Cl]_{Nat}$ leaching fluxes were the lowest and $[Cl]_{Tracer}$ leaching fluxes were the highest. However, these differences were very small. At 30 cm depth, the greatest annual leaching flux difference between optimization strategies was 0.1 kg ha^{-1} $year^{-1}$ for Ca (in 2001), 0.5 kg ha^{-1} $year^{-1}$ for NO_3 (in 1999) and 2.6 kg ha^{-1} $year^{-1}$ for Cl (in 1999). At 80 cm depth, the greatest annual leaching flux difference between optimization strategies was 0.1 kg ha^{-1} $year^{-1}$ for Ca (in 2001), 0.3 kg ha^{-1} $year^{-1}$ for NO_3 (in 1999) and 3.1 kg ha^{-1} $year^{-1}$ for Cl (in 2001). For all three optimization strategies, the model uncertainty associated with predicted annual leaching fluxes was very similar between optimizations but decreased with depth. For example, the Ca leaching flux uncertainty ranged from 10 to 44% at 30 cm depth and from 4 to 19% at 80 cm depth. Uncertainties varied quite substantially between the different solutes. The highest model uncertainties were observed for NO_3: relative standard deviations ranged from 10 to 103% at 30 cm depth and from 18 to 72% at 80 cm depth.

The annual leaching flux was calculated by coupling zero tension lysimeter solutions to the modeled preferential water flow and tension-cup lysimeters solutions to the modeled matric flow (ZTL + TCL) Table 6). Ca, NO_3 and Cl concentrations varied quite substantially between soil solution types (ZTL or TCL) (Figure S2), most especially

Table 5. Annual Water Drainage Output and Associated Uncertainties (SD: Standard Deviation; RSD: Relative Standard Deviation) Predicted by the WatFor Model for the Three Optimization Strategies (θ, [Cl]Nat and [Cl]Tracer) and the Five Depths (10, 30, 80 and 120)

Optimization	Year	10 cm				30 cm				55 cm				80 cm				120 cm			
		Mean mm year^{-1}	SD mm year^{-1}	RSD %		Mean mm year^{-1}	SD mm year^{-1}	RSD %		Mean mm year^{-1}	SD mm year^{-1}	RSD %		Mean mm year^{-1}	SD mm year^{-1}	RSD %		Mean mm year^{-1}	SD mm year^{-1}	RSD %	
θ	1999	560	6	1.1	a	510	7	1.4	a	463	9	1.9	a	398	10	2.5	a	370	11	3.0	a
	2000	700	9	1.3	a	646	10	1.5	a	587	10	1.6	a	571	12	2.1	ab	564	12	2.1	a
	2001	514	6	1.5	a	455	9	1.9	a	404	7	1.8	a	342	7	2.1	a	333	6	1.9	a
	2002	570	8	1.4	a	518	11	2.1	a	458	9	2.0	a	431	9	2.1	ab	411	10	2.4	a
	2003	323	5	1.5	a	272	6	2.2	a	221	6	2.7	a	158	6	3.6	a	144	5	3.3	a
	2004	379	7	1.7	a	327	7	2.2	a	284	6	2.0	a	230	5	2.1	a	205	5	2.3	a
$[Cl]_{Nat}$	1999	55	6	1.0	a	501	5	1.0	a	458	5	1.1	a	392	5	1.4	a	365	6	1.7	a
	2000	679	10	1.4	b	601	8	1.3	b	575	7	1.3	a	565	7	1.2	a	562	7	1.2	a
	2001	501	8	1.7	a	433	9	2.0	b	389	5	1.4	b	335	4	1.2	a	333	4	1.2	a
	2002	551	9	1.7	b	480	10	2.0	b	443	8	1.7	a	420	6	1.5	a	405	6	1.5	a
	2003	314	5	1.6	a	258	5	1.9	b	216	5	2.5	a	155	5	3.1	a	144	4	2.6	a
	2004	364	7	2.0	b	307	7	2.2	b	267	4	1.6	b	221	4	1.6	a	200	4	2.1	a
$[Cl]_{Tracer}$	1999	581	6	1.0	b	540	6	1.1	b	483	4	0.9	b	416	3	0.7	b	388	4	1.1	b
	2000	739	8	1.0	c	716	8	1.1	c	612	7	1.2	b	578	6	1.0	b	563	5	0.9	a
	2001	546	6	1.1	b	509	8	1.7	c	438	7	1.6	c	367	4	1.0	b	341	3	1.0	b
	2002	612	5	0.8	c	589	6	1.0	c	493	9	1.9	b	441	7	1.5	b	422	5	1.2	b
	2003	349	5	1.3	b	307	4	1.4	c	244	6	2.3	b	178	5	2.7	b	151	4	2.7	a
	2004	414	5	1.1	c	383	6	1.4	c	319	7	2.1	c	258	3	1.3	b	230	4	1.6	b

Significant differences between the optimization strategies are indicated with different letters.

for Ca. At 30 cm depth, the annual leaching flux was on average greater (1.6 fold for both Ca and Cl) and smaller (0.5 fold for NO_3) for the ''ZTL + TCL'' method compared to the ''TCL'' method. At 80 cm depth, for Cl, the annual leaching fluxes were very similar between the ''TCL'' and ''ZTL + TCL'' methods. For NO_3, the leaching fluxes were on average greater for the ''ZTL + TCL'' method (respectively, from 1.6 to 2.9 fold); however, differences were not significant due to the elevated standard deviations (Table 6). Finally, for Ca, the leaching flux was also greater (from 2.0 to 3.4 fold) for the ''ZTL + TCL'' method and these differences were significant.

Discussion

The three calibration methods were compared according to the uncertainty range of predicted model parameters, the repeatability of the model parameter uncertainty ranges, the goodness of fit between modeled and measured data and finally the uncertainty in the predicted water drainage flux. Though the results showed only small variations in the modeled water drainage (Table 5) and nutrient leaching outputs (Table 6), differences between calibration methods were sufficiently significant and enable one to discuss the efficiency of each method according to the objective of the modeling exercise:

1. Daily soil moisture calibration dataset was the most efficient to model distribution of water uptake and water drainage in the soil profile (Table 4; Figure 3)
2. The experimental water tracing calibration dataset was the most efficient to model the partitioning of matrix and preferential water flow in the soil profile (Table 4; Figure 5)
3. The natural variations of chloride concentrations in soil solution was the most versatile calibration dataset and was efficient for modeling both preferential water flow, water uptake distribution and water drainage in the soil profile (Table 4).

Distribution of Water Availability and Uptake in the Soil

Although the performance of the WatFor model at reproducing soil moisture variations in the soil was similar (Table 4) and satisfactory (mostly within the measurement uncertainty) for all three calibration strategies (Figure 3), soil drying and wetting dynamics were, unsurprisingly, best reproduced by the θ strategy. Interestingly, the goodness of fit between modeled and measured soil moisture obtained with the $[Cl]_{Nat}$ strategy was very similar to the θ strategy because monitoring soil moisture at experimental or monitoring sites is expensive, such datasets are often unavailable and hydrological models can only be calibrated using the natural variations of chloride concentration in the soil solution (Jonard and others 2012; Zanchi and others 2014; Yu and others 2016). The results of this study suggest that $[Cl]_{Nat}$ datasets may be used to calibrate water balance models when no soil moisture monitoring data are available.

The goodness of fit of the $[Cl]_{Tracer}$ strategy for the soil moisture dataset was poorer than the two other strategies (Table 4; Figure 3). Soil drying dynamics in the upper part of the soil profile were slower and less intense than observed in the measured data and the two other optimization strategies. These differences are explained by different estimated water uptake distribution parameters in the $[Cl]_{Tracer}$ strategy (Table 3). Although the uncertainty range for the root distribution parameters was lowest for the chloride tracer optimization strategy (Table 3), the repeatability of the upper and lower boundary estimates was also lower compared to the two other strategies. Water tracing experiments may thus not be best adapted to estimate the water uptake distribution parameters. This discrepancy between optimization strategies may be explained by the fact that the data from the water tracing experiment only covered ca 1.5 hydrological years (March 2006–December 2007). This single tracing experiment may not be representative of the inter-annual climate variability observed over the 1999–2005 period. In the θ and $[Cl]_{Nat}$ strategies, model parameters were optimized over a range of years (1999–2004) that (1) did not overlap with the chloride tracing experiment (2006–2007) and (2) varied from very dry (for example, 2003 with 780 mm of rainfall) to very wet (for example, 2000 with 1295 mm of rainfall), while 2006 and 2007 were average years with 992 mm and 1195 mm of rainfall, respectively.

In the context of climate change, the resistance and resilience of forest stands to drought is an important concern in the forest management community. Severe and/or repetitive droughts may lead to a reduction of forest productivity (Piovesan and others 2008; Kirchen and others 2017), tree mortality (Hülsmann and others 2016) and in certain cases forest dieback (Bréda and

Table 6. Annual Ca, NO_3 and Cl Leaching Fluxes at 30 cm and 80 cm Depth and Associated Uncertainties (SD: Standard Deviation; RSD: Relative Standard Deviation) Predicted by the WatFor Model for the Three Optimization Strategies

Calculation method	Year	*n*	30 cm depth												80 cm depth											
			Ca				NO_3				Cl				Ca				NO_3				Cl			
			Mean	SD	RSD		Mean	SD	RSD		Mean	SD	RSD		Mean	SD	RSD		Mean	SD	RSD		Mean	SD	RSD	
θ	1999	11	1.8	0.2	10.1	a	5.8	0.6	10.3	a	49.3	2.0	4.1	a	1.1	0.2	18.6	a	7.5	1.4	18.0	a	37.5	1.3	3.4	ab
TCL	2000	11	1.1	0.5	42.3	a	1.8	1.3	72.6	a	23.1	2.2	9.6	a	1.0	0.1	9.6	a	1.3	0.4	33.4	a	49.0	1.6	3.2	a
	2001	12	0.8	0.3	35.2	a	5.1	2.7	53.1	a	14.5	0.9	6.2	a	0.6	0.1	12.0	a	0.9	0.3	29.6	a	31.2	0.7	2.3	a
	2002	9	0.9	0.2	27.0	a	1.2	1.2	96.8	a	30.8	1.6	5.2	a	0.9	0.0	4.1	a	0.4	0.2	45.8	a	51.8	5.2	10.0	a
	2003	8	0.2	0.1	44.3	a	0.2	0.2	68.9	a	7.1	0.5	7.2	a	0.4	0.0	9.6	a	0.1	0.0	69.3	a	23.9	1.3	5.6	a
	2004	6	0.1	0.0	24.4	a	0.2	0.1	39.2	a	6.4	0.5	7.7	a	0.4	0.1	14.8	a	0.1	0.1	55.7	a	26.2	1.1	4.1	A
$[Cl]_{Nat}$	1999	11	1.8	0.2	10.1	a	5.7	0.6	10.1	a	48.5	2.0	4.2	a	1.0	0.2	17.6	a	7.3	1.3	18.0	a	37.0	1.1	2.9	a
TCL	2000	11	1.1	0.4	41.5	a	1.9	1.2	64.7	a	22.6	2.1	9.3	a	1.0	0.1	9.2	a	1.2	0.4	32.7	a	48.4	1.4	2.8	a
	2001	12	0.9	0.3	35.2	a	5.0	2.6	52.5	a	14.3	0.9	6.1	a	0.6	0.1	12.3	a	0.9	0.2	28.5	a	30.5	0.5	1.7	a
	2002	9	0.9	0.3	27.9	a	1.3	1.3	103.0	a	30.6	1.8	5.8	a	0.9	0.0	3.9	a	0.4	0.2	46.4	a	51.6	5.2	10.1	a
	2003	8	0.2	0.1	42.7	a	0.2	0.2	73.0	a	7.0	0.5	7.3	a	0.4	0.0	9.1	a	0.1	0.0	71.7	a	23.5	1.3	5.6	a
	2004	6	0.1	0.0	26.3	a	0.2	0.1	40.1	a	6.2	0.5	7.6	a	0.4	0.1	14.0	a	0.1	0.1	56.6	a	26.2	1.0	3.7	a
$[Cl]_{Tracer}$	1999	11	1.9	0.2	9.6	a	6.2	0.6	9.9	a	51.0	2.1	4.2	a	1.1	0.2	17.8	a	7.6	1.4	18.6	a	39.5	1.0	2.5	b
TCL	2000	11	1.2	0.5	39.3	a	1.9	1.5	74.9	a	23.9	2.2	9.3	ab	1.0	0.1	9.1	a	1.3	0.4	32.1	a	49.2	1.4	2.9	a
	2001	12	1.0	0.3	34.8	a	5.2	2.9	54.9	a	16.1	1.0	6.0	a	0.7	0.1	11.4	a	0.9	0.2	27.7	a	33.6	0.5	1.4	b
	2002	9	1.0	0.3	26.2	a	1.6	1.3	86.6	a	32.4	1.6	5.1	a	0.9	0.0	3.5	a	0.4	0.2	47.1	a	52.7	5.1	9.7	a
	2003	8	0.2	0.1	40.1	a	0.2	0.2	68.1	a	7.3	0.5	7.4	a	0.5	0.0	9.0	a	0.1	0.0	64.5	a	26.0	1.3	4.9	a
	2004	6	0.1	0.0	26.8	a	0.2	0.1	40.3	a	6.6	0.5	8.1	a	0.4	0.1	14.5	a	0.1	0.1	57.0	a	26.0	0.9	3.4	a
$[Cl]_{Nat}$	1999	11	3.4	2.2	64.3	a	1.9	1.6	88.6	b	32.9	2.6	8.0	b	3.3	1.3	39.5	b	20.2	15.6	77.4	a	35.4	2.2	6.1	a
ZTL + TCL	2000	11	2.1	1.5	72.9	a	2.4	6.1	257.7	a	28.0	2.6	9.5	b	3.3	1.1	31.8	b	3.5	3.3	92.9	a	47.0	2.3	4.9	a
	2001	12	1.0	0.5	50.2	a	1.8	3.6	202.9	a	30.0	1.9	6.2	b	1.7	0.6	33.9	b	2.5	2.2	89.7	a	30.1	1.3	4.4	a
	2002	9	0.8	0.8	99.9	a	0.2	0.2	122.7	a	22.9	3.1	13.7	b	2.4	0.8	31.8	b	1.3	1.5	120.9	a	49.1	5.3	10.8	a
	2003	8	0.1	0.1	68.7	a	0.1	0.1	109.5	a	8.6	1.8	20.5	a	1.3	0.5	38.7	b	0.2	0.4	169.3	a	22.6	1.4	6.1	a
	2004	6	0.4	0.3	82.7	a	0.1	0.1	95.8	a	22.5	2.8	12.6	b	0.8	0.3	38.7	b	0.2	0.2	115.4	a	25.8	1.3	4.9	a

n represents the number of months of available soil solution concentration data for the calculation. TCL indicates that the leaching flux was calculated by coupling 100% of the water drainage flux with TCL solution concentration data. ZTL + TCL indicates that the leaching flux was calculated by coupling the modeled preferential water drainage flux with ZTL solution concentration data and the modeled matric water drainage flux with TCL solution concentration data. Significant differences between the optimization strategies are indicated with different letters.

others 2006) particularly in European Beech (*Fagus sylvatica* L.) stands (Lebourgeois and others 2005; H. and others 2006). The response of tree growth to drought has been shown to vary between beech stands probably in relation to soil properties and soil hydrology (Lebourgeois and others 2005; Pascale and others 2007). Forest soil hydrological models such as WatFor enable to predict soil water availability as a function of climatic variables, study the water uptake strategies of tree species (Granier and others 1999) and therefore help understand and predict the consequences of climate change of forest ecosystems. Coupling forest growth and mortality models with hydrological models may contribute to explain the observed temporal and spatial variability of ecosystem response to droughts (Hülsmann and others 2016) and improve our understanding of the relation between water availability in the soil, reduced forest productivity and increased tree mortality. Because modeled predictions of reduced forest productivity and/or tree mortality and/or forest dieback in the context of climate change greatly influence future forest policies and forest management (Allen and others 2010), it is essential to evaluate and report the uncertainties associated with model simulations (Beven 1989). This is particularly true because singular extreme drought events are likely to have a stronger impact on tree species distribution limits than long-term trends (Rasztovits and others 2014). It may also be noted that model uncertainty assessment is essential to compare the performance of different models in a robust manner and hence improve existing models.

The results of this study show that the GLUE procedure is an efficient method to partly automate the model calibration procedure and to estimate uncertainties associated with model simulation of soil water content (Figure 3). Our results suggest that soil moisture datasets are the best choice to calibrate hydrological models in the scope of predicting water availability in the soil over time and that natural variations of chloride concentration in soil solution may be used as a substitute calibration dataset or validation dataset. This particular result opens the possibility of modeling forest soil hydrology, and thus coupling soil hydrology models with forest productivity and tree mortality models, in a broader range of monitored ecosystems for which no soil moisture data are available (for example, the European ICP Forest Network).

Water Transfer Velocity and Importance of Preferential Water Flow in the Soil Profile

In many study cases, water tracing experiments have provided conclusive evidence of the occurrence of preferential flow paths in the soil and are a preferred tool to characterize and quantify these flow paths (Deeks and others 2008; Allaire and others 2009; Legout and others 2009a; van der Heijden and others 2013; Yan and Zhao 2016). In agreement, the results of the GLUE procedure suggest that experimental water tracing data are the most relevant of the three strategies to estimate preferential flow generation model parameters. The topsoil field capacity infiltration parameter boundaries strongly converged to a range of likely values from 6.6 to 6.9 mm day^{-1} (Table 3). These threshold values are within the 0.1 to 1 mm h^{-1} given for topsoils of loam and clay texture in Jarvis (2007). Additionally, although the range of likely values for the wilting point infiltration parameter remained broad, the $[Cl]_{Tracer}$ strategy yielded the best estimation for this parameter from a convergence and repeatability point of view.

The modeling results also show that the performance of the model at reproducing the water tracing experiment with the $[Cl]_{Nat}$ calibration strategy was very close to the $[Cl]_{Tracer}$ strategy. This suggests that $[Cl]_{Nat}$ may also be used to estimate preferential flow generation model parameters. For both calibration strategies, the modeled proportion of preferential flow was higher than estimated from the water tracing experiment data: approximately 17% (Legout and others 2009a). This difference is likely explained by the simplistic manner in which preferential flow paths and preferential flow generation is represented in the WatFor model. Water balance models need to better represent these processes, most especially when preferential flow represents an important proportion of the water transfer in the soil profile.

The soil moisture optimization strategy failed to reproduce the elution of the chloride tracer in the soil profile probably because of the high uncertainties associated with preferential flow generation parameters (Table 3). When preferential flow is either not or poorly represented in hydrological models, the modeled vertical transfer of the water tracer is likely to be too fast because, when preferential flow occurs, part of the percolation flux does not participate in the piston effect on tracer displacement (van der Heijden and others 2013).

Model Uncertainty in Relation to Soil Profile Depth

The water uptake distribution in the soil profile is a key model parameter to estimate when the objective of the modeling approach is to predict soil moisture and/or water drainage in the upper part of a soil profile. The $[Cl]_{Tracer}$ calibration strategy is a good illustration of this: small differences in water uptake distribution (Table 3) caused important differences in the water drainage flux (Table 5). However, at the bottom of the soil profile, differences of annual water drainage flux between the three calibration strategies were small. In addition, for all three calibration strategies, the uncertainties associated with the predicted water drainage flux decreased from the topsoil to the bottom of the soil profile. This result may appear counterintuitive because the water drainage flux at the bottom of the profile is the result of the sum of the water mass balance in each soil layer and thus the sum of uncertainties in each soil layer. However, in the model, 100% of the water uptake is assigned to the soil profile. From a water mass balance perspective, differences in water uptake distribution may generate differences in water drainage in the upper part of the soil profile but these differences are evened out over the whole profile. Consequently, in this study case, the uncertainty in the modeled water drainage flux at the rooting zone boundary is much less sensitive to the water uptake distribution parameter. It must, however, be noted that the climate at the Fougères site is oceanic and wet. Under dryer climates, it is most likely that the modeled water drainage flux at the rooting zone boundary would be more sensitive to the water uptake distribution parameter.

Nutrient Fluxes in the Soil Profile

The results of this study showed that the optimization/calibration dataset selection did not have a significant effect on the estimated nutrient leaching fluxes in the soil profile (Table 6). To our knowledge only a few studies have estimated nutrient leaching flux uncertainty values and these studies focused on watershed stream flow. At the Hubbard Brook experimental forest, Campbell and others (2016) reported uncertainty estimates for the Ca flux in the streams of two paired watersheds (5.1% and 6.9%) and Yanai and others (2015) reported uncertainty estimates for NO_3: from 5 to 30%. Uncertainty in nutrient export in stream flow is likely to be smaller than at the rooting zone boundary because, in the former, ''discharge is used as a multiplier to obtain the flux and can be precisely observed'' (Appling and others 2015). The uncertainty associated with nutrient leaching was smaller than expected. This is most likely due to the fact that most of the estimated annual nutrient leaching flux occurred during winter periods during which uncertainties associated with both water drainage flux and the spatial variability of measured concentrations were low (data not shown). Although we cannot generalize the results of this case study, they suggest that, depending on (1) the nutrient considered and (2) the relative importance of the leaching flux in the input–output budget, the leaching flux may represent an important source of uncertainty in input–output budgets calculated for the soil profile.

Uncertainties in the calculation methodology (*for example,* coupling of drainage water with measured soil solution concentrations) may cause higher levels of uncertainty for the leaching flux estimates. The importance of the water sampling system (tension cup and zero tension lysimeters) with regard to the objectives of ecosystem studies has been discussed by numerous previous studies (Hendershot and Courchesne 1991; Marques and others 1996; Weihermuller and others 2007; Legout and others 2009a; Watmough and others 2013). Zero tension lysimeters are commonly considered to be best adapted to compute nutrient leaching fluxes in the soil profile and thus input–output budgets. However, zero tension lysimeters solutions are not representative of all mobile soil water (Weihermuller and others 2007): weakly bound soil water, which is mobile in the soil through matric flow (Legout and others 2009a; van der Heijden and others 2013), is not collected by these lysimeters. On the other hand, tension-cup lysimeters mainly collect weakly bound water but have also been shown to collect preferential flow water (Legout and others 2009b). Therefore, it may not be concluded which water type chemistry is the most adequate to estimate nutrient leaching fluxes but at sites where preferential flow plays an important role in the soil water fluxes, this additional uncertainty should be taken into account.

This uncertainty associated with water type used to calculate the nutrient leaching flux was assessed for the $[Cl]_{Nat}$ strategy (Table 6). The results show a potentially important solute-dependent effect of the calculation methodology on nutrient leaching estimates. We cannot conclude from this data which calculation methodology is best adapted to compute input–output budgets but our results highlight the importance of the water type selection on the nutrient leaching flux estimate and the

importance of better understanding how the different water types interact and transfer in the soil profile.

Using Natural Chloride Concentration Datasets to Calibrate Water Balance Models

The results of this study showed that the $[Cl]_{Nat}$ strategy was the most versatile of the three optimization strategies tested and enabled to satisfactorily reproduce both soil moisture, natural variations of chloride concentrations and the elution of a chloride tracer in the soil profile. This result was not expected given the rather low variability over time and/or seasonality of measured chloride concentrations in soil solution (Figure 4). This was particularly true in the deeper soil layers where the measured variability over time and/or seasonality was often within spatial variability. Model parameter optimization therefore mainly relied on reproducing the mean concentration level and the trends in the dataset.

At this site, it appears that natural variations of chloride concentrations in this European beech plot are mainly controlled by water pools and fluxes in the soil with little influence of the biological cycle of chloride. This is supported by the chloride input–output budget calculated for this plot which was close to zero (on average 2 ± 9 kg ha^{-1} year^{-1} over the 1999–2004 period). However, in some reported cases, the biological cycling of chloride in forest ecosystems (Svensson and others 2012; Montelius and others 2015) has been shown to greatly influence chloride fluxes in the soil profile thus questioning its' use as an ideal tracer of water. In such cases, natural variations of chloride concentrations may still be used to calibrate water balance models but precautions must be taken when no other calibration dataset is available. Hydrological models may also be used as an indicator of the influence of the biological cycle on the geochemical cycle of chloride.

Conclusion

The choice of the dataset used to calibrate water balance model parameters is not trivial and influences model parameter estimates and model outputs. The selection of the calibration dataset should be adapted to the objectives of modeling approach. The modeling data of this study support all three hypotheses that this study aimed to test. The soil moisture dataset was the most adequate to model water availability and water uptake distribution in the soil profile (H1). The water tracing experimental dataset was the most adequate to model preferential water flow paths (H2). Natural variations of chloride concentrations in the soil solution was also a very relevant dataset to calibrate the water balance model (H3) and provided the most versatile calibration of the WatFor model satisfactorily reproducing all three datasets (daily soil moisture measurements, monthly measurements of chloride concentrations in soil solution, and the elution of a concentrated chloride tracer).

This modeling approach suggests that model parameter uncertainties cause only little uncertainty in the modeled water drainage flux at the rooting zone boundary. Uncertainty in nutrient leaching is, however, more important due to the high spatial variability of soil solution concentrations. Finally, our results also show potentially high uncertainties may be associated with our incomplete knowledge of the chemical composition (water types) and the different (preferential and matric) components of the water drainage flux.

Acknowledgements

We would like to thank all the technicians without whom this project would not have been possible, in particular C. Antoine, L. Gelhaye and S. Bienaimé from INRA Nancy. This work was financed by the EFPA department (INRA), the GIP ECOFOR and by the Office National des Forêts in the context of one of the Environmental Research sites on ''Lowland beech'' part of F-ore-T network. The UR-1138 INRA—*Biogéochimie des Ecosystèmes Forestiers* is supported by a grant overseen by the French National Research Agency (ANR) as part of the ''Investissements d'Avenir'' program (ANR-11-LABX-0002-01, Lab of Excellence ARBRE).

References

Adriaenssens S, Staelens J, Baeten L, Verstraeten A, Boeckx P, Samson R, Verheyen K. 2013. Influence of canopy budget model approaches on atmospheric deposition estimates to forests. Biogeochemistry 116:215–29.

Akelsson C, Westling H, Sverdrup H, Gundersen P. 2007. Nutrient and carbon budgets in forest soils as decision support in sustainable forest management. Forest Ecology And Management 238:167–74.

Allaire SE, Roulier S, Cessna AJ. 2009. Quantifying preferential flow in soils: A review of different techniques. Journal of Hydrology 378:179–204.

Allen CD, Macalady AK, Chenchouni H, Bachelet D, McDowell N, Vennetier M, Kitzberger T, Rigling A, Breshears DD, Hogg EH, Gonzalez P, Fensham R, Zhang Z, Castro J, Demidova N, Lim J-H, Allard G, Running SW, Semerci A, Cobb N. 2010. A global overview of drought and heat-induced tree mortality

reveals emerging climate change risks for forests. Forest Ecology And Management 259:660–84.

Appling AP, Leon MC, McDowell WH. 2015. Reducing bias and quantifying uncertainty in watershed flux estimates: the R package loadflex. Ecosphere 6:1–25.

Aussenac G. 1968. Interception des précipitations par le couvert forestier. Ann. Sci. forest 25:135–56.

Baize D, Girard MC. 1998. A sound reference base for soils: the ''Référentiel Pédologique''. Paris: INRA. p 324p.

Bedison JE, Johnson AH. 2010. Seventy-Four Years of Calcium Loss from Forest Soils of the Adirondack Mountains, New York. Soil Science society of America Journal 74:2187–95.

Beven K. 1989. Changing ideas in hydrology — The case of physically-based models. Journal of Hydrology 105:157–72.

Beven K, Binley A. 1992. The future of distributed models: Model calibration and uncertainty prediction. Hydrological processes 6:279–98.

Beven K, Binley A. 2014. GLUE: 20 years on. Hydrological processes 28:5897–918.

Bormann FH, Likens GE. 1967. Nutrient cycling. Science 155:424–9.

Boxman AW, Peters RCJH, Roelofs JGM. 2008. Long term changes in atmospheric N and S throughfall deposition and effects on soil solution chemistry in a Scots pine forest in the Netherlands. Environmental Pollution 156:1252–9.

Bréda N, Huc R, Granier A, Dreyer E. 2006. Temperate forest trees and stands under severe drought: a review of ecophysiological responses, adaptation processes and long-term consequences. Ann. For. Sci. 63:625–44.

Campbell JL, Yanai RD, Green MB, Likens GE, See CR, Bailey AS, Buso DC, Yang DQ. 2016. Uncertainty in the net hydrologic flux of calcium in a paired-watershed harvesting study. Ecosphere 7:15.

Christiansen JR, Elberling B, Jansson PE. 2006. Modelling water balance and nitrate leaching in temperate Norway spruce and beech forests located on the same soil type with the Coup-Model. Forest Ecology And Management 237:545–56.

Cooper DM. 2005. Evidence of sulphur and nitrogen deposition signals at the United Kingdom Acid Waters Monitoring Network sites. Environmental Pollution 137:41–54.

Court M, van der Heijden G, Didier S, Nys C, Richter C, Pousse N, Saint-André L, Legout A. 2018. Long-term effects of forest liming on mineral soil, organic layer and foliage chemistry: Insights from multiple beech experimental sites in Northern France. Forest Ecology And Management 409:872–89.

Dambrine E, Vega JA, Taboada T, Rodriguez L, Fernandez C, Macias F, Gras JM. 2000. Budgets of mineral elements in small forested catchments in Galicia (NW Spain). Annals of forest science 57:23–38.

Deeks LK, Bengough AG, Stutter MI, Young IM, Zhang XX. 2008. Characterisation of flow paths and saturated conductivity in a soil block in relation to chloride breakthrough. Journal of Hydrology 348:431–41.

Gérard F, Tinsley M, Mayer KU. 2004. Preferential Flow Revealed by Hydrologic Modeling Based on Predicted Hydraulic Properties. Soil Science society of America Journal 68:1526–38.

Giesler R, LundstrÖM US, Grip H. 1996. Comparison of soil solution chemistry assessment using zero-tension lysimeters or centrifugation. European Journal of Soil Science 47:395–405.

Granier A, Bréda N, Biron P, Villette S. 1999. A lumped water balance model to evaluate duration and intensity of drought constraints in forest stands. Ecological Modelling 116:269–83.

H. R, F. L, A. P, F. B, S. F, S. BR, A. G. 2006. Physiological Responses of Forest Trees to Heat and Drought. Plant Biology 8: 556–71

Hendershot WH, Courchesne F. 1991. Comparison of soil solution chemistry in zero tension and ceramic-cup tension lysimeters. Journal of Soil Science 42:577–83.

Hodson ME, Langan SJ. 1999. A long-term soil leaching column experiment investigating the effect of variable sulphate loads on soil solution and soil drainage chemistry. Environmental Pollution 104:11–19.

Hülsmann L, Bugmann HKM, Commarmot B, Meyer P, Zimmermann S, Brang P. 2016. Does one model fit all? Patterns of beech mortality in natural forests of three European regions. Ecological applications 26:2465–79.

Huntington TG, Hooper RP, Johnson CE, Aulenbach BT, Cappellato R, Blum AE. 2000. Calcium depletion in a southeastern United States forest ecosystem. Soil Science society of America Journal 64:1845–58.

IUSS Working Group WRB. 2007. World refernce base for soil resources 2006, First Update 2007. FAO, Rome No: World Soil Resources Reports. p 103.

Jarvis NJ. 2007. A review of non-equilibrium water flow and solute transport in soil macropores: principles, controlling factors and consequences for water quality. European Journal of Soil Science 58:523–46.

Johnson DW, Todd DE. 1998. Harvesting effects on long-term changes in nutrient pools of mixed oak forest. Soil Science Society of America Journal 62:1725–35.

Johnson DW, Todd DE Jr, Trettin CF, Mulholland PJ. 2008. Decadal Changes in Potassium, Calcium, and Magnesium in a Deciduous Forest Soil. Soil Science society of America Journal 72:1795–805.

Jonard M, Fürst A, Verstraeten A, Thimonier A, Timmermann V, Potočić N, Waldner P, Benham S, Hansen K, Merilä P, Ponette Q, de la Cruz AC, Roskams P, Nicolas M, Croisé L, Ingerslev M, Matteucci G, Decinti B, Bascietto M, Rautio P. 2015. Tree mineral nutrition is deteriorating in Europe. Global Change Biology 21:418–30.

Jonard M, Legout A, Nicolas M, Dambrine E, Nys C, Ulrich E, van der Perre R, Ponette Q. 2012. Deterioration of Norway spruce vitality despite a sharp decline in acid deposition: a long-term integrated perspective. Global Change Biology 18:711–25.

Kavetski D, Kuczera G, Franks SW. 2006. Bayesian analysis of input uncertainty in hydrological modeling: 1. Theory. Water resources research 42:9.

Kirchen G, Calvaruso C, Granier A, Redon P-O, Van der Heijden G, Bréda N, Turpault M-P. 2017. Local soil type variability controls the water budget and stand productivity in a beech forest. Forest Ecology And Management 390:89–103.

Kuczera G, Parent E. 1998. Monte Carlo assessment of parameter uncertainty in conceptual catchment models: the Metropolis algorithm. Journal of Hydrology 211:69–85.

Lebourgeois F, Bréda N, Ulrich E, Granier A. 2005. Climate-tree-growth relationships of European beech (Fagus sylvatica L.) in the French Permanent Plot Network (RENECOFOR). Trees 19:385–401.

Legout A, Legout C, Nys C, Dambrine E. 2009a. Preferential flow and slow convective chloride transport through the soil of a forested landscape (Fougères, France). Geoderma 151:179–90.

Legout A, Nys C, Picard JF, Turpault MP, Dambrine E. 2009b. Effects of storm Lothar (1999) on the chemical composition of soil solutions and on herbaceous cover, humus and soils (Fougeres, France). Forest Ecology And Management 257:800–11.

Legout A, van der Heijden G, Jaffrain J, Boudot J-P, Ranger J. 2016. Tree species effects on solution chemistry and major element fluxes: A case study in the Morvan (Breuil, France). Forest Ecology And Management 378:244–58.

Legout A, Walter C, Nys C. 2008. Spatial variability of nutrient stocks in the humus and soils of a forest massif (Fougeres, France). Annals of forest science 65:10.

Marques R, Ranger J, Gelhaye D, Pollier B, Ponette Q, Goedert O. 1996. Comparison of chemical composition of soil solutions collected by zero-tension plate lysimeters with those from ceramic-cup lysimeters in a forest soil. European Journal of Soil Science 47:407–17.

Montelius M, Thiry Y, Marang L, Ranger J, Cornelis J-T, Svensson T, Bastviken D. 2015. Experimental Evidence of Large Changes in Terrestrial Chlorine Cycling Following Altered Tree Species Composition. Environmental Science & Technology 49:4921–8.

Neitsch SL, Arnold JG, Kiniry JR, Williams JR. 2011. Soil and water assessment tool theoretical documentation version 2009. Texas Water Resources Institute.

Norton SA, Young HE. 1976. Forest biomass utilization and nutrient budgets. Oslo biomass studies. Papers presented during the meeting of S4.01 [Mensuration, Growth and Yield] in Oslo, Norway, June 22, 1976. XVIth International Congress of IUFRO.: 55–73.

Öberg G, Holm M, Sandén P, Svensson T, Parikka M. 2005. The Role of Organic-matter-bound Chlorine in the Chlorine Cycle: A Case Study of the Stubbetorp Catchment, Sweden. Biogeochemistry 75:241–69.

Ogee J, Brunet Y, Loustau D, Berbigier P, Delzon S. 2003. MuSICA, a CO2, water and energy multilayer, multileaf pine forest model: evaluation from hourly to yearly time scales and sensitivity analysis. Global Change Biology 9:697–717.

Pascale W, Harald B, Andreas R. 2007. Radial growth responses to drought of Pinus sylvestris and Quercus pubescens in an inner-Alpine dry valley. Journal of Vegetation Science 18:777–92.

Piovesan G, Biondi F, Di Filippo A, Alessandrini A, Maugeri M. 2008. Drought-driven growth reduction in old beech (*Fagus sylvatica L.*) forests of the central Apennines. Italy. Global Change Biology 14:1265–81.

Ranger J, Turpault M-P. 1999. Input-output nutrient budgets as a diagnostic tool for sustainable forest management. Forest Ecology And Management 122:139–54.

Rasztovits E, Berki I, Mátyás C, Czimber K, Pötzelsberger E, Móricz N. 2014. The incorporation of extreme drought events improves models for beech persistence at its distribution limit. Annals of forest science 71:201–10.

Reuss JO, Johnson DW. 1986. Acid deposition and the acidification of soils and waters. New York: Springer-Verlag 119p.

Rivera D, Rivas Y, Godoy A. 2015. Uncertainty in a monthly water balance model using the generalized likelihood uncertainty estimation methodology. Journal of Earth System Science 124:49–59.

Shen ZY, Chen L, Chen T. 2012. Analysis of parameter uncertainty in hydrological and sediment modeling using GLUE method: a case study of SWAT model applied to Three Gorges Reservoir Region, China. Hydrology and Earth System Sciences 16:121–32.

Simunek J, Jarvis NJ, van Genuchten MT, Gardenas A. 2003. Review and comparison of models for describing non-equilibrium and preferential flow and transport in the vadose zone. Journal of Hydrology 272:14–35.

Svensson T, Lovett GM, Likens GE. 2012. Is chloride a conservative ion in forest ecosystems? Biogeochemistry 107:125–34.

Sverdrup H, Thelin G, Robles M, Stjernquist I, Sörensen J. 2006. Assesing nutrient sustainability of forest production for different tree species considering Ca, Mg, K, N and P at Björnstorp Estate, Sweden. Biogeochemistry 81:219–38.

Toutain F. 1965. Etude des sols et des eaux de la forêt de Fougères. Université de Rennes.

van der Heijden G, Belyazid S, Dambrine E, Ranger J, Legout A. 2017. NutsFor a process-oriented model to simulate nutrient and isotope tracer cycling in forest ecosystems. Environmental Modelling & Software 95:365–80.

van der Heijden G, Legout A, Nicolas M, Ulrich E, Johnson DW, Dambrine E. 2011. Long-term sustainability of forest ecosystems on sandstone in the Vosges Mountains (France) facing atmospheric deposition and silvicultural change. Forest Ecology And Management 261:730–40.

van der Heijden G, Legout A, Pollier B, Bréchet C, Ranger J, Dambrine E. 2013. Tracing and modeling preferential flow in a forest soil — Potential impact on nutrient leaching. Geoderma 195–196:12–22.

Van Vliet-Lanoë B, Pellerin J, Helluin M. 1995. Morphogenèse-pédogenèse: les héritages du dernier cycle glaciaire en forêt de Fougères (Ille et Vilaine, France). Geomorph. N. F. 39:489–510.

Vuorenmaa J. 2004. Long-term changes of acidifying deposition in Finland (1973-2000). Environmental Pollution 128:351–62.

Vuorenmaa J, Augustaitis A, Beudert B, Clarke N, de Wit HA, Dirnbock T, Frey J, Forsius M, Indriksone I, Kleemola S, Kobler J, Kram P, Lindroos AJ, Lundin L, Ruoho-Airola T, Ukonmaanaho L, Vana M. 2017. Long-term sulphate and inorganic nitrogen mass balance budgets in European ICP Integrated Monitoring catchments (1990-2012). Ecological Indicators 76:15–29.

Watmough SA, Koseva I, Landre A. 2013. A Comparison of Tension and Zero-Tension Lysimeter and PRS™ Probes for Measuring Soil Water Chemistry in Sandy Boreal Soils in the Athabasca Oil Sands Region, Canada. Water, Air, & Soil Pollution 224:1663.

Weihermuller L, Siemens J, Deurer M, Knoblauch S, Rupp H, Gottlein A, Putz I. 2007. In situ soil water extraction: A review. Journal of environmental quality 36:1735–48.

Yan JL, Zhao WZ. 2016. Characteristics of preferential flow during simulated rainfall events in an arid region of China. Environmental Earth Sciences 75:12.

Yanai RD, Tokuchi N, Campbell JL, Green MB, Matsuzaki E, Laseter SN, Brown CL, Bailey AS, Lyons P, Levine CR, Buso DC, Likens GE, Knoepp JD, Fukushima K. 2015. Sources of uncertainty in estimating stream solute export from headwater catchments at three sites. Hydrological processes 29:1793–805.

Yang J, Reichert P, Abbaspour KC, Xia J, Yang H. 2008. Comparing uncertainty analysis techniques for a SWAT application to the Chaohe Basin in China. Journal of Hydrology 358:1–23.

Yu L, Belyazid S, Akselsson C, van der Heijden G, Zanchi G. 2016. Storm disturbances in a Swedish forest—A case study comparing monitoring and modelling. Ecological Modelling 320:102–13.

Zanchi G, Belyazid S, Akselsson C, Yu L. 2014. Modelling the effects of management intensification on multiple forest services: a Swedish case study. Ecological Modelling 284:48–59.

Zheng Y, Keller AA. 2007. Uncertainty assessment in watershed-scale water quality modeling and management: 1. Framework and application of generalized likelihood uncertainty estimation (GLUE) approach. Water resources research 43:13.